

SPIN-ORBIT INTERACTION IN NEUTRON STAR/MAIN-SEQUENCE BINARIES AND  
IMPLICATIONS FOR PULSAR TIMING

DONG LAI

Theoretical Astrophysics, 130-33, California Institute of Technology, Pasadena, CA 91125; dong@tapir.caltech.edu

LARS BILDSTEN

Department of Physics and Department of Astronomy, University of California, Berkeley, CA 94720; bildsten@fire.berkeley.edu

AND

VICTORIA M. KASPI<sup>1</sup>

IPAC/Caltech/Jet Propulsion Laboratory, Pasadena, CA 91125; vicky@ipac.caltech.edu

Received 1995 March 22; accepted 1995 April 28

## ABSTRACT

The spin-induced quadrupole moment of a rapidly rotating star changes the orbital dynamics in a binary system, giving rise to advance (or regression) of periastron and precession of the orbital plane. We show that these effects are important in the recently discovered radio pulsar/main-sequence star binary system PSR J0045–7319 and reliably account for the observed peculiar timing residuals. Precise measurements of the apsidal motion and orbital plane precession can yield valuable information on the internal structure and rotation of the star. The detection of orbital precession implies that the spin of the companion star is not aligned with the orbital angular momentum and suggests that the supernova gave the pulsar a kick out of the original orbital plane. Tidal excitation of  $g$ -mode oscillations in the PSR J0045–7319 system induces an orbital period change of order  $|\Delta P_{\text{orb}}/P_{\text{orb}}| \sim 10^{-6}$  at each periastron passage, but the secular trend depends on the radiative damping time of the  $g$ -modes. We also discuss the spin-orbit coupling effects for the accreting X-ray pulsars and the other known radio pulsar/main-sequence binary, PSR B1259–63.

*Subject headings:* binaries: close — pulsars: individual (PSR J0045–7319, PSR B1259–63) — stars: neutron — stars: oscillations — stars: rotation

## 1. INTRODUCTION

The discovery of radio pulsars in binary systems with massive main-sequence stars (PSR B1259–63, Johnston et al. 1992, 1994; PSR J0045–7319, Kaspi et al. 1994) makes it possible to measure hydrodynamical effects on the pulsar orbit. Indeed, the detection of large ( $\pm 30$  ms) *frequency-independent* timing residuals from PSR J0045–7319 (Kaspi et al. 1995a) has motivated our consideration of the dynamical effects caused by the spin-induced quadrupole moment on the stellar companion. This is expected to be the dominant effect, as massive main-sequence stars are fast rotators and typically have rotation periods on the order of days (Jaschek & Jaschek 1987). We show that the spin-orbit coupling in these systems is indeed significant and leads to both apsidal motion and precession of the orbital plane that can account for the timing residuals seen in PSR J0045–7319.

The information learned from pulsar/main-sequence binaries will complement the studies of double main-sequence binaries, many of which have large enough quadrupoles (either from tides or fast rotation) to cause measurable apsidal motion in their eccentric orbits. As reviewed by Claret & Gimenez (1993), the apsidal motion is combined with information on the stellar masses, radii, and spins to yield the apsidal constant,  $k$ , which is a dimensionless measure of the density concentration of the stellar interior. These measurements compare favorably with those expected from theoretical stellar structure models (see Claret & Gimenez 1993 for the few exceptions). The pulsar systems considered here are most sensitive to the spin-induced

quadrupole, permitting better studies of the orientation and magnitude of the spin of the stellar companion. Both these quantities are important to constrain and/or measure in the context of mass transfer prior to the supernova and “kicks” during the neutron star birth.

We start in § 2 by explaining why the spin-induced quadrupole moment is important for these systems and then summarize the full equations for the precession and apsidal motion, correcting some previous typographical errors. We then show in § 3 that the induced time delay is large and easily measurable for the two radio pulsars under consideration, PSR J0045–7319 and PSR B1259–63. We demonstrate that this effect is present in the timing data of PSR J0045–7319. In particular, the unusual residuals observed by Kaspi et al. (1995a) are the result of fitting a purely Keplerian orbit to irregularly sampled data in which apsidal advance and orbital precession are present. Section 4 contains simple estimate of the dynamical tidal effect that might prove important. We show that tidal excitation of high-order gravity modes in the companion of PSR J0045–7319 near periastron can yield significant changes in the orbital period and eccentricity which may be measurable. We conclude in § 5 by outlining the prospects for constraining the system parameters of PSR J0045–7319 and the possibilities for similar measurements in accreting X-ray pulsars.

## 2. SPIN-ORBIT COUPLING IN BINARY SYSTEMS

The neutron star’s gravitational field couples to both the tide-induced quadrupole and the spin-induced quadrupole of the stellar companion. We begin by comparing the relative magnitudes of these two effects. The tidal bulge on the stellar

<sup>1</sup> Hubble Fellow.

companion has a height  $h \sim M_p R_c^4 / (M_c r^3)$ , where  $M_c$  and  $R_c$  are the companion mass and radius,  $M_p$  is the pulsar (neutron star) mass, and  $r$  is the instantaneous center of mass separation. The tidal quadrupole is then roughly  $Q_{\text{tide}} \sim k M_c R_c^2 (h/R_c) \sim k M_p R_c^2 (R_c/r)^3$ . We compare this to the quadrupole induced by rotation at angular velocity,  $\Omega_s = 2\pi/P_s$ ,  $Q_{\text{spin}} \sim k M_c R_c^2 (\Omega_s^2 R_c^3 / G M_c)$ . At periastron, the ratio of these two is

$$\frac{Q_{\text{spin}}}{Q_{\text{tide}}} \sim \left( \frac{P_{\text{orb}}}{P_s} \right)^2 \frac{(M_p + M_c)}{M_p} (1 - e)^3, \quad (1)$$

where  $P_{\text{orb}}$  and  $e$  are the orbital period and eccentricity. Equation (1) shows that when  $\Omega_s$  is larger than the orbital angular velocity at periastron,  $\Omega_{\text{orb},p} = \Omega_{\text{orb}}(1+e)^{1/2}/(1-e)^{3/2}$ , the spin-induced quadrupole effect is more important than the tidal effect. Binary systems containing early-type stars (in particular, those with convective cores and radiative envelopes) with orbital periods longer than 2–3 days are not expected to circularize and synchronize appreciably in a time comparable to the main-sequence life span, at least when the eccentricities are not too large (Zahn 1977, 1984). Both PSR B1259–63 and PSR J0045–7319 are of this type and, as we describe in § 3, are timed with sufficient accuracy for these effects to be measurable.

### 2.1. Spin-Induced Distortion

The quadrupole from the rotational distortion of the finite-sized companion is specified by the difference between the moments of inertia about the spin-axis,  $I_3$ , and an orthogonal axis,  $I_1$ . Claret & Gimenez (1992) calculated the moment of inertia for slowly rotating main-sequence stars. We incorporate their results by introducing a parameter  $\lambda$ , whose value is close to unity, so that  $I_3 \equiv 0.1\lambda M_c R_c^2$  (the parameter  $\lambda$  also accounts for the increase of the equatorial radius of the rotating star, which can be as large as  $3R_c/2$  near the maximum rotation rate). The quadrupole from the rotational distortion of the star is proportional to the spin squared. Following the conventional definition of the apsidal motion constant  $k$  (Cowling 1938; Schwarzschild 1958), we write

$$I_3 - I_1 = \frac{2}{3} k M_c R_c^2 \hat{\Omega}_s^2, \quad (2)$$

where  $\hat{\Omega}_s$  is the dimensionless spin  $\hat{\Omega}_s \equiv \Omega_s / (G M_c / R_c^3)^{1/2}$  of the companion. For stars with uniform density,  $k = \frac{3}{4}$ . For the  $M_c \approx 10 M_\odot$  main-sequence star of interest here,  $k \approx 0.01$ , depending on the stellar age (Schwarzschild 1958; Claret & Gimenez 1992).

### 2.2. Spin-induced Apsidal Motion and Orbital Precession

Because of the spin-induced quadrupole moment, the additional  $1/r^3$  potential term between the components leads to apsidal motion (advance or regression of the longitude of periastron) and, when the spin angular momentum  $\mathbf{S}$  is not aligned with the orbital angular momentum  $\mathbf{L}$ , a precession of the orbital plane. The general expressions for the rates of apsidal motion and orbital precession have been derived by Smarr & Blandford (1976) and Kopal (1978, p. 232) using standard celestial mechanics perturbation theory. In the coordinates of Figure 1, the rate of change of the dynamical longitude of periastron (measured from the ascending node in the invariable plane perpendicular to  $\mathbf{J} = \mathbf{L} + \mathbf{S}$ ),  $\chi$ , is given by

$$\dot{\chi} = \frac{3\pi(I_3 - I_1)}{M_c a^2 (1 - e^2) P_{\text{orb}}} \left( 1 - \frac{3}{2} \sin^2 \theta + \frac{1}{2} \sin 2\theta \cot \theta_c \right), \quad (3)$$

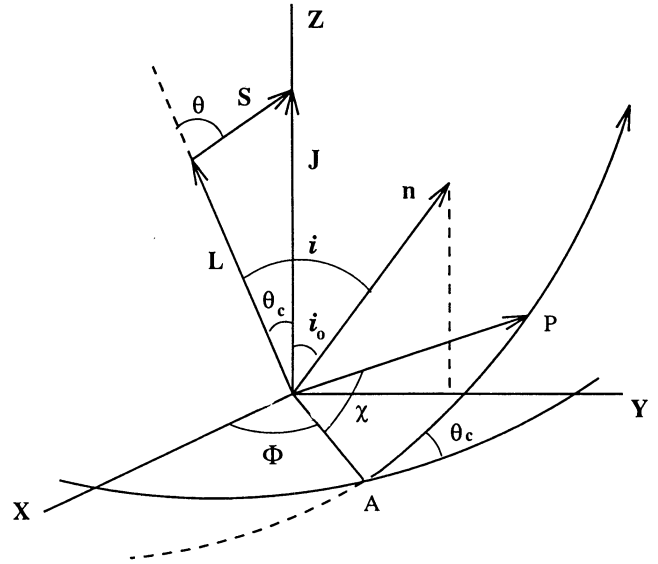


FIG. 1.—Binary geometry and the definitions of different angles. The invariable plane ( $X$ - $Y$ ) is perpendicular to the total angular momentum vector  $\mathbf{J} = \mathbf{L} + \mathbf{S}$ , and the line-of-sight unit vector  $\mathbf{n}$  lies in the  $Y$ - $Z$  plane, making an angle  $i_0$  with  $\mathbf{J}$ . The inclination of the orbit with respect to the invariable plane is  $\theta_c$  (which is also the precession cone angle of  $\mathbf{L}$  around  $\mathbf{J}$ ), while the orbital inclination with respect to the plane of the sky is  $i$ . The angle between  $\mathbf{L}$  and  $\mathbf{S}$  is  $\theta$ . The orbital plane intersects the invariable plane at ascending node  $A$ , with longitude  $\Phi$  measured in the invariable plane ( $\Phi$  is also the phase of the orbital plane precession). The dynamical longitude of periastron (point  $P$ ), measured in the orbital plane, is  $\chi$ . The observational longitude of periastron is  $\omega$  (not shown in the figure).

where  $a$  is the semimajor axis of the (relative) orbit,  $\theta$  is the angle between  $\mathbf{L}$  and  $\mathbf{S}$ , and  $\theta_c$  is the angle between  $\mathbf{L}$  and  $\mathbf{J}$ .

The orbital plane precession rate  $\Omega_{\text{prec}} = \dot{\Phi}$  (see Fig. 1) can be obtained more directly by calculating the interaction torque between the stars. We have

$$\begin{aligned} \Omega_{\text{prec}} &= -\frac{3GM_p(I_3 - I_1) \cos \theta}{2a^3(1 - e^2)^{3/2}} \frac{\mathbf{J}}{SL} \\ &= -\frac{3\pi(I_3 - I_1)}{M_c a^2 (1 - e^2)^2 P_{\text{orb}}} \left( \frac{\sin \theta \cos \theta}{\sin \theta_c} \right) \hat{\mathbf{J}}, \end{aligned} \quad (4)$$

where the minus sign implies that  $\mathbf{L}$  precesses in a direction opposite to  $\mathbf{J}$ , and we have used  $L = [GM_p^2 M_c^2 a(1 - e^2)/M_i]^{1/2}$  for the Keplerian orbital angular momentum. In the limit of small mass ratio  $M_p \ll M_c$  and  $S \equiv |\mathbf{S}| \gg L \equiv |\mathbf{L}|$ , equations (3) and (4) reduce to the rates of apsidal motion and orbital precession for the Earth-satellite system (Goldstein 1980). By contrast, for binary pulsars of interest in this paper,  $L \gg S$ . Using the moment of inertia  $I_3 \equiv 0.1\lambda M_c R_c^2$  with the quadrupole from equation (2), we obtain

$$\Omega_{\text{prec}} \approx -\Omega_{\text{orb}} \frac{10kM_p}{\lambda(M_c M_t)^{1/2}} \left( \frac{R_c}{a} \right)^{3/2} \frac{\hat{\Omega}_s \cos \theta}{(1 - e^2)^{3/2}}, \quad (5)$$

<sup>2</sup> This can be derived following the perturbation procedure of § 11-3.C of Goldstein (1980, p. 512), except that here the action variables are  $J_1 = 2\pi L \cos \theta_c$ ,  $J_2 = 2\pi L$ , and note that the perturbation Hamiltonian (11-58) depends on  $\theta$  (or  $i$  in Goldstein's notation), the angle between  $\mathbf{L}$  and  $\mathbf{S}$ . Note that in eq. (3.10) of Smarr & Blandford (1976),  $\sin^2(\delta + \theta)$  should be  $\sin 2(\delta + \theta)$ ; also in eq. (11-60) of Goldstein (1980), the factor  $(1 - e^2)^{-1}$  should be  $(1 - e^2)^{-2}$ .

where  $M_t = M_p + M_c$ . The angle of the precession cone (i.e., the angle between  $\mathbf{L}$  and  $\mathbf{J}$ ) is simply  $\theta_c \simeq S \sin \theta/L$  in the  $L \gg S$  limit.

The above derivation assumes that the companion star behaves as a rigid body. One might be concerned that fluid stars respond to external forces differently than a rigid object (Smarr & Blandford 1976; Papaloizou & Pringle 1982). This is by no means a resolved issue, although it seems unlikely that deviation from rigid body behavior is large since the tidal distortion of the star is small compared to the rotational distortion. The observations of these pulsars may well provide information on this subtlety.

### 2.3. Effects on the Observables

The apsidal motion and orbital plane precession change  $\omega$ , the observational longitude of periastron (measured from the ascending node in the plane of the sky), and  $i$ , the orbital inclination angle (the angle between  $\mathbf{L}$  and  $\mathbf{n}$ , the unit vector along the line of sight). Let  $i_0$  be the angle between  $\mathbf{J}$  and  $\mathbf{n}$  (see Fig. 1), in which case the observational angles  $\omega$  and  $i$  are related to  $\chi$  and  $\Phi$  by:

$$\sin \omega = \frac{1}{\sin i} [(\sin \theta_c \cos i_0 + \cos \theta_c \sin i_0 \cos \Phi) \sin \chi + \sin i_0 \cos \chi \sin \Phi], \quad (6)$$

$$\cos i = -\sin \theta_c \sin i_0 \cos \Phi + \cos i_0 \cos \theta_c.$$

For  $L \gg S$  or  $\theta_c \ll 1$ , these reduce to  $\omega \simeq \chi + \Phi$  and  $i \simeq i_0 + \theta_c \cos \Phi$ . Using equations (2), (3), and (4), we then have

$$\dot{\omega} \simeq \frac{3\pi(I_3 - I_1)}{M_c a^2(1 - e^2)P_{\text{orb}}} \left(1 - \frac{3}{2} \sin^2 \theta\right) \simeq \Omega_{\text{orb}} \frac{kR_c^2 \hat{\Omega}_s^2}{a^2(1 - e^2)^2} \left(1 - \frac{3}{2} \sin^2 \theta\right), \quad (7)$$

and

$$\frac{di}{dt} \simeq \frac{3\pi(I_3 - I_1)}{M_c a^2(1 - e^2)P_{\text{orb}}} \sin \theta \cos \theta \sin \Phi \simeq \Omega_{\text{orb}} \frac{kR_c^2 \hat{\Omega}_s^2}{a^2(1 - e^2)^2} \sin \theta \cos \theta \sin \Phi. \quad (8)$$

Thus, for typical  $\theta$  and  $\Phi$ , the numerical value of  $di/dt$  is comparable to that of  $\dot{\omega}$ . Note that the observed apsidal motion is an advance for  $\sin \theta < (2/3)^{1/2}$  and a regression in the opposite case. In addition, twice in one precession cycle, at  $\Phi = 0$  and  $\pi$  (i.e., when  $\mathbf{J}$ ,  $\mathbf{L}$ , and  $\mathbf{n}$  lie in the same plane), the rate  $di/dt$  for the change of the orbital inclination angle is identically zero.

### 3. SPIN-ORBIT EFFECTS ON BINARY PULSAR TIMING

We now consider the effects of spin-orbit coupling on the timing of the two binary pulsar systems with main-sequence star companions. The orbital motion gives rise to a delay of  $T(t) = \mathbf{r}_p \cdot \mathbf{n}/c = r_p(t) \sin \Psi(t) \sin i(t)/c$  in the pulse arrival time, where  $\mathbf{r}_p = \mathbf{r}M_c/(M_p + M_c)$  is the pulsar position vector. The orbital phase (or true anomaly)  $\Psi(t)$  measured from the observational ascending node is given by  $\Psi(t) = \Psi(t)_K + \dot{\omega}t$ , where  $\Psi(t)_K$  is the Keplerian value. The longitude of periastron  $\omega(t)$  and the orbital inclination angle  $i(t)$  vary according to equations (7) and (8), with the precession phase given by  $\Phi(t) = \Omega_{\text{prec}} t + \Phi_0$ .

We are interested in the residual  $\delta T(t) \equiv r_p \cdot \mathbf{n}/c - (r_p \cdot \mathbf{n}/c)_K$  of the time delay compared to the Keplerian value. For  $t \ll 1/|\Omega_{\text{prec}}|$  and  $t \ll 1/|\dot{\omega}|$ , we have  $\delta T = \delta T_{\text{aps}} + \delta T_{\text{prec}}$ , where the contributions from apsidal motion and orbital plane precession are given by (assuming  $\delta T = 0$  at  $t = 0$ )

$$\delta T(t)_{\text{aps}} \simeq \frac{r_p(t)}{c} \sin i_0 \cos \Psi(t) \dot{\omega} t, \quad (9)$$

$$\delta T(t)_{\text{prec}} \simeq \frac{r_p(t)}{c} \cos i_0 \sin \Psi(t) \frac{di}{dt} t.$$

Clearly, the residual resulting from the neglect of varying  $\omega$  and  $i$  in the timing model increases with  $t$  and is modulated by the orbital motion.<sup>3</sup> Equations (9) are the leading order corrections for this effect and are valid for timescales much less than the precession period, which is  $\sim 300$  yr for PSR J0045–7319 (see § 3.1). The next order terms are about a factor of  $\dot{\omega}t$  or  $(di/dt)t$  smaller and have different dependences on  $i$  and  $\Psi$ . The accumulation of accurate timing data over a longer baseline will further constrain the system.

#### 3.1. PSR J0045–7319

Radio timing observations by Kaspi et al. (1994) of the 0.93 s pulsar PSR J0045–7319 have identified it to be in an eccentric ( $e = 0.8080$ ) 51.17 day orbit having projected semimajor axis  $a_p \sin i/c = 174$  s. They made optical observations in the direction of the pulsar and found a B1 V star with  $B = 16.03$  and  $V = 16.19$  which showed no evidence for emission lines. Combining the effective temperature ( $T_{\text{eff}} \approx 2.4 \times 10^4$  K) and reddening ( $A_V \approx 0.27$ ) with the observed colors gives  $R_c \simeq (6.4 \pm 0.5) R_\odot$  ( $d/59$  kpc). The optical radial velocity measurements of the B star fix its mass to be  $(8.8 \pm 1.8) M_\odot$  for  $M_p = 1.4 M_\odot$  and give  $i = 44^\circ \pm 5^\circ$  (Bell et al. 1995). This then yields  $a \simeq 126 R_\odot \simeq 20R_c$ . The rotational velocity  $v_{\text{rot}} \sin \theta_{sn} \simeq 113 \pm 10$  km  $s^{-1}$  (where  $\theta_{sn}$  is the angle between  $\mathbf{S}$  and  $\mathbf{n}$ ) obtained from spectral line broadening (Bell et al. 1995) corresponds to  $\hat{\Omega}_s \simeq 0.22/\sin \theta_{sn}$ , consistent with a rapid rotation near breakup,  $\hat{\Omega}_{s,\text{max}} \simeq 0.5$ . The ratio of  $\Omega_s$  and the angular velocity at periastron  $\Omega_{\text{orb},p}$  is  $\simeq 1.1/\sin \theta_{sn}$ , confirming that the system is not synchronized. Equations (5), (7), and (8) then give

$$\Omega_{\text{prec}} \simeq -1.9 \times 10^{-2} \lambda^{-1} \left(\frac{k}{0.01}\right) \left(\frac{20R_c}{a}\right)^{3/2} \times \left(\frac{\hat{\Omega}_s}{0.5}\right) \cos \theta \text{ rad yr}^{-1},$$

$$\dot{\omega} \simeq 2.3 \times 10^{-3} \left(\frac{k}{0.01}\right) \left(\frac{20R_c}{a}\right)^2 \left(\frac{\hat{\Omega}_s}{0.5}\right)^2 \times \left(1 - \frac{3}{2} \sin^2 \theta\right) \text{ rad yr}^{-1},$$

$$\frac{di}{dt} \simeq 2.3 \times 10^{-3} \left(\frac{k}{0.01}\right) \left(\frac{20R_c}{a}\right)^2 \left(\frac{\hat{\Omega}_s}{0.5}\right)^2 \times \sin \theta \cos \theta \sin \Phi \text{ rad yr}^{-1}.$$

<sup>3</sup> Note that for very eccentric systems, the changes in  $\omega$  and  $i$  occur mainly near periastron, rather than accumulating uniformly throughout the orbital period. We neglect this finer point in eq. (9).



The timing residual  $\Delta T$  accumulated in one orbit is estimated by setting  $r_p \simeq 2a_p$  and  $t \simeq P_{\text{orb}}/2$  in equation (9), giving

$$\begin{aligned}\Delta T_{\text{aps}} &\simeq \frac{a_p \sin i}{c} \dot{\omega} P_{\text{orb}} \\ &\simeq 56 \left( \frac{k}{0.01} \right) \left( \frac{20R_c}{a} \right)^2 \left( \frac{\hat{\Omega}_s}{0.5} \right)^2 \left( 1 - \frac{3}{2} \sin^2 \theta \right) \text{ms}, \\ \Delta T_{\text{prec}} &\simeq \frac{a_p \cos i}{c} \frac{di}{dt} P_{\text{orb}} \\ &\simeq 56 \left( \frac{k}{0.01} \right) \left( \frac{20R_c}{a} \right)^2 \left( \frac{\hat{\Omega}_s}{0.5} \right)^2 \left( \frac{\cos i}{\sin i} \sin \theta \cos \theta \sin \Phi \right) \text{ms}.\end{aligned}\quad (11)$$

The modulated residual in just one orbit is thus comparable to the residuals found by Kaspi et al. (1995a).

There are other effects that can also give rise to secular changes in  $\omega$  and  $i$ . The standard formula for the apsidal motion resulting from static tide (Cowling 1938; Schwarzschild 1958) gives  $\dot{\omega}_{\text{tide}} \simeq 1.3 \times 10^{-4} (k/0.01) (20R_c/a)^5 \text{ rad yr}^{-1}$ , about an order of magnitude smaller than the spin-induced  $\dot{\omega}$ . This secular trend is degenerate with the spin-induced quadrupole effect. Tidal effects do not produce changes in the orbital inclination angle. General relativity also induces periastron advance (Landau & Lifshitz 1962)  $\dot{\omega}_{\text{gr}} \simeq 6.7 \times 10^{-5} \text{ rad yr}^{-1}$ , comparable to the tidal effect. The geodetic precession of the companion star's spin (Barker & O'Connell 1975; note that the spin angular momentum of the pulsar is much smaller than that of the companion) results in an orbital precession  $\dot{\Omega}_{\text{prec,gr}} \simeq 5.9 \times 10^{-6} \text{ rad yr}^{-1}$ , 3 orders of magnitude smaller than the Newtonian spin-induced quadrupole effect.

### 3.2. PSR B1259–63

This 47.76 ms pulsar is in an eccentric orbit with a Be star companion with  $P_{\text{orb}} = 1236$  days,  $e = 0.8698$ , and  $a_p \sin i/c = 1296$  s (Johnston et al. 1992, 1994). The optical data for this emission-line star are still inadequate to place strong constraints on the spectral type and hence radius of the star, so we will use the fiducial values chosen by Johnston et al. (1994),  $R_c = 6 R_{\odot}$  and  $M_c = 10 M_{\odot}$ . For  $M_p = 1.4 M_{\odot}$ , we obtain  $a = 1091 R_{\odot} = 182R_c$ . For typical values ( $\lambda \simeq 1$ ,  $k \simeq 0.01$ , and  $\hat{\Omega}_s \simeq 0.5$ ) we obtain  $\dot{\Omega}_{\text{prec}} \simeq -4.1 \times 10^{-5} \cos \theta \text{ rad yr}^{-1}$ ,  $\dot{\omega} \simeq 2.4 \times 10^{-6} (1 - 3/2 \sin^2 \theta) \text{ rad yr}^{-1}$ , and  $di/dt \simeq 2.4 \times 10^{-6} \sin \theta \cos \theta \sin \Phi \text{ rad yr}^{-1}$ . The timing residual accumulated in one orbit is given by

$$\begin{aligned}\Delta T_{\text{aps}} &\simeq 10 \left( \frac{k}{0.01} \right) \left( \frac{182R_c}{a} \right)^2 \left( \frac{\hat{\Omega}_s}{0.5} \right)^2 \left( 1 - \frac{3}{2} \sin^2 \theta \right) \text{ms}, \\ \Delta T_{\text{prec}} &\simeq 10 \left( \frac{k}{0.01} \right) \left( \frac{182R_c}{a} \right)^2 \left( \frac{\hat{\Omega}_s}{0.5} \right)^2 \\ &\quad \times \left( \frac{\cos i}{\sin i} \sin \theta \cos \theta \sin \Phi \right) \text{ms}.\end{aligned}\quad (12)$$

Thus,  $\Delta T$  can potentially affect the timing parameters for this system as well. Indeed, using a pure Keplerian model for the system resulted in substantial systematic timing residuals (Johnston et al. 1994; Manchester et al. 1995). From our estimate above, it is clear that these residuals may well have a significant contribution from the unfitted  $\dot{\omega}$  and  $di/dt$ . A full

understanding of this system is complicated by the dispersion and radio eclipse caused by the wind from the Be star.

The tide-induced apsidal motion  $\dot{\omega}_{\text{tide}} \simeq 2.7 \times 10^{-10} (k/0.01) (182R_c/a)^5 \text{ rad yr}^{-1}$ , as well as the general relativistic effects, are completely negligible for this system.

Note that the expressions given in § 2 describe the *secular* change of the orbit, i.e., they are obtained by orbital averaging. To model closely sampled timing data spanning only a few orbits, as in PSR B1259–63, a numerical integration of the orbit with the perturbing potential may be required.

### 3.3. Data Fitting and the Observed Residual in PSR J0045–7319

Using multifrequency radio timing observations of PSR J0045–7319, Kaspi et al. (1995a) showed that the observed barycentric pulse arrival times deviated significantly from those expected from a pure Keplerian orbit. In particular, they found significant *frequency-independent* timing residuals for a  $\sim 10$  day duration around periastron. These residuals showed systematic variations on timescales of a few days after subtraction of a Keplerian orbital fit to the entire 3.3 yr data span. The residuals from two periastron observations separated by 11 orbits showed very different trends, inconsistent with a simple error in any of the Keplerian parameters. They noted that such residuals were unlike those of any other pulsar, isolated or binary.

We show here that the unusual PSR J0045–7319 residuals can be explained by the relatively long-term dynamical effects described above, in spite of the former's apparent short-timescale variations. To do this, we simulated timing observations for a binary pulsar which has Keplerian parameters similar to those of PSR J0045–7319, but which in addition has two post-Keplerian parameters, the apsidal advance  $\dot{\omega}$  and a time-variable projected semimajor axis  $\dot{x}$ , where  $x = a_p \sin i$ . In the simulation,  $x$  and  $\omega$  were incremented by 0.0044 lt-sec and  $0^{\circ}0035$  per orbit at periastron, which gave the best match to the observed residuals. These numbers correspond to  $\dot{\omega} \simeq 4.4 \times 10^{-4} \text{ rad yr}^{-1}$  and  $di/dt \simeq 1.8 \times 10^{-4} \text{ rad yr}^{-1}$ , consistent with equation (16). The actual fit to the data from PSR J0045–7319 and the implications for that source in particular will be discussed elsewhere (Kaspi et al. 1995b).

The simulated data were then fitted with a pure Keplerian orbit, holding all post-Keplerian parameters fixed at zero, thus simulating the analysis done by Kaspi et al. (1995a). The residuals for this fit are shown in the upper panel of Figure 2. The effect of the post-Keplerian parameters is obvious as an orbital period modulation of increasing amplitude relative to the fitting epoch (see eq. [9]). The fitted Keplerian parameters are biased away from the assumed values because of the least-squares fitting procedure; indeed, the fitted solution shown in the figure has “spikes” for this reason. Next, using the same set of simulated arrival times, we selected those that coincide with actual observations of PSR J0045–7319 at the Parkes Observatory, in order to simulate the sampling interval used by Kaspi et al. (1995a) in their timing analysis. Again we fit a simple Keplerian orbit, holding all post-Keplerian parameters fixed at zero. The resulting post-fit residuals are shown in the middle panel of Figure 2. Close-up views of the two epochs of periastron investigated by Kaspi et al. are shown in the bottom panels; a comparison with the data indicates that this model closely mimics the observed trends. Thus, we have shown that the unusual residuals for PSR J0045–7319 can be explained as being a result of fitting a purely Keplerian orbit to infrequently

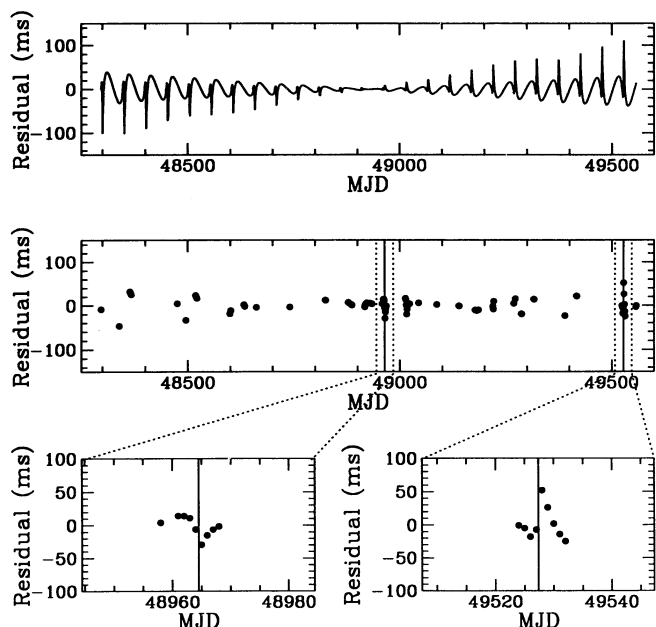


FIG. 2.—Simulated pulse arrival times for PSR J0045–7319. *Top*: residuals from a fit of a pure Keplerian orbit to fake pulse arrival time data (“measured” daily for four years) for a binary pulsar like PSR J0045–7319 in which apsidal advance and orbital plane precession are important. *Middle*: residuals from a fit of this fake data sampled only at those epochs coinciding with actual observations of the pulsar. The two vertical solid lines show epochs of periastron separated by 11 orbits. *Bottom*: close-ups of those epochs; the observed trends in the residuals are similar to those observed by Kaspi et al. (1995a).

and irregularly sampled data in which post-Keplerian apsidal advance and orbital plane precession are significant.

#### 4. POSSIBLE ORBITAL PERIOD CHANGE RESULTING FROM DYNAMICAL TIDE

The spin-induced quadrupole effects (and the standard tide-induced apsidal motion) discussed in the previous sections assume that at a given binary separation the star relaxes instantaneously to the equilibrium state. However, dynamical tidal effects associated with the excitation of  $g$ -modes in the companion star result in energy and angular momentum transfer between the star and the orbit during each periastron passage, therefore changing in the orbital period and eccentricity.<sup>4</sup>

The energy transfer  $\Delta E$  during each periastron passage can be estimated with the formalism of Press & Teukolsky (1977), who considered tidal excitations for a parabolic orbit.<sup>5</sup> In the quadrupole order, this is given by

$$\Delta E \sim -\frac{GM_p^2}{R_c} \left(\frac{R_c}{r_{\min}}\right)^6 T_2(\eta), \quad (13)$$

where  $r_{\min}$  is the binary separation at periastron,  $\eta = (M_c/M_p)^{1/2}(r_{\min}/R_c)^{3/2}$  is the ratio of the time for periastron passage and the stellar dynamical time, and the dimensionless function  $T_2(\eta)$  (defined in Press & Teukolsky 1977) involves

<sup>4</sup> Mass loss from the companion star can in principle induce similar changes in the orbit. However, the absence of eclipses or orbital phase-dependent DM variations constrains the ionized mass-loss rate  $\dot{M}_c \gtrsim 10^{-10} M_\odot \text{ yr}^{-1}$  for PSR J0045–7319 (Kaspi et al. 1994, 1995a), suggesting that the dynamical importance of the mass loss is small.

<sup>5</sup> This formalism is also reasonably accurate for highly elliptic orbits. This is because most of the energy transfer takes place near periastron, where the kinetic energy and potential energy  $\sim GM_p M_c / r_{\min}$  are much larger than the binding energy  $GM_p M_c / (2a)$ , and the orbit resembles a parabolic trajectory.

$l = 2$  nonradial stellar oscillation modes and the orbital trajectory. The resulting fractional change of the orbital size is simply  $\Delta a/a = -\Delta E/E$ , and the orbital period change is given by

$$\frac{|\Delta P_{\text{orb}}|}{P_{\text{orb}}} = \frac{3|\Delta a|}{2a} \sim 3 \frac{M_p}{M_c} \left(\frac{R_c}{a}\right)^5 (1-e)^{-6} T_2(\eta). \quad (14)$$

The angular momentum transferred during periastron is of order  $\Delta L \sim \Delta E(GM_c/R_c^3)^{-1/2}$ ; thus,  $|\Delta L/L|$  is typically negligible compared to  $|\Delta E/E|$ . The resulting change in orbital eccentricity is then  $\Delta e \simeq (\Delta a/a)(1-e^2)/(2e)$ .

To estimate the importance of the dynamical tidal effects, we compare  $\Delta a/a$  with the fractional change (resulting from the static tide) of  $\omega$  in one orbit  $\Delta\omega/(2\pi) = \dot{\omega}_{\text{tide}} P_{\text{orb}}/(2\pi)$ . For PSR J0045–7319, using the parameters of § 3.1, we have  $\eta \simeq 7.0$  and  $T_2(\eta) \simeq 3.5 \times 10^{-4}$  for an  $n = 3$  polytrope with adiabatic index  $\Gamma_1 = 5/3$  (e.g., Lee & Ostriker 1986), where most contributions to  $T_2(\eta)$  come from  $g$ -modes of radial order 5–9. This gives  $|\Delta a/a| \sim 0.1\Delta\omega/(2\pi)$ , implying that the perturbation resulting from energy transfer is much smaller than the tide-induced apsidal motion and is therefore even smaller than the spin effects discussed in §§ 2–3. This estimate agrees with the more detailed study by Kumar, Ao, & Quataert (1995). The orbital period change caused by the energy transfer is given by  $|\Delta P_{\text{orb}}|/P_{\text{orb}} \sim 10^{-6}$ , more than an order of magnitude larger than the measurement accuracy of  $P_{\text{orb}}$  attained over many orbits (Kaspi et al. 1995a). The associated eccentricity change  $|\Delta e| \sim 10^{-7}$  will be more difficult to measure. For PSR B1259–63, again using the parameters of § 3.2, we have  $\eta \simeq 108$ , for which  $T_2(\eta)$  is extremely small, and the dynamical tidal effects are therefore completely negligible.<sup>6</sup>

It is important to note that the actual values and signs of  $\Delta P_{\text{orb}}$  and  $\Delta e$  depend on the damping of the tidally excited  $g$ -modes. Depending on detailed stellar models, the radiative damping time for  $g$ -modes in an early-type main-sequence star is of order 100 yr, although some  $g$ -modes can be damped in less than 1 yr (e.g., Unno et al. 1979, pp. 205–217). If the damping time  $t_{\text{damp}}$  is much longer than the orbital period, the energy transfer for an elliptical orbit will depend on the phases of the oscillations of different modes and vary (both in magnitude and sign) from one passage to another. In this case, equation (14) only represents the typical magnitude of  $\Delta P_{\text{orb}}$  during each passage, not a steady  $\dot{P}_{\text{orb}}$ ; the *averaged* long-term orbital decay rate is expected to be of order  $-|\Delta P_{\text{orb}}|/t_{\text{damp}}$ . On the other hand, if the damping time  $t_{\text{damp}}$  is much shorter than the orbital period, the energy transfer near periastron is a one-way process, i.e., only from the orbit to the star. Therefore,  $\Delta P_{\text{orb}}/P_{\text{orb}}$  and  $\Delta e$  represent steady negative values, i.e., the orbit decays and circularizes. If such a short damping timescale indeed applies to the high-order  $g$ -modes excited in PSR J0045–7319, the orbital decay can be observable in the timing data. A more accurate calculation of this effect is complicated by the rapid rotation of the B star, which changes the  $g$ -mode structure when the rotation frequency is comparable to the  $g$ -mode frequencies.

#### 5. DISCUSSION

Smarr & Blandford (1976) first discussed the Newtonian spin-orbit effects in the context of PSR B1913+16. That companion turned out to be a neutron star, which renders these

<sup>6</sup> Kochanek (1993) has previously discussed the dynamical tidal effects in the context of PSR B1259–63. However, the observational data available then did not allow him to draw any firm conclusion.

Newtonian effects completely negligible and facilitates excellent tests of general relativity (e.g., Taylor & Weisberg 1989). The recent discovery of two radio pulsar/main-sequence star binaries, PSR J0045–7319 and PSR B1259–63, finally allows for measurements of hydrodynamical effects in binary pulsar systems. In this paper we have shown that the Newtonian spin-orbit coupling is particularly important in PSR J0045–7319 and PSR B1259–63 systems.

### 5.1. Constraints on the Binary Systems and Evolution

When the spin-induced quadrupole is the dominant effect, measuring  $\dot{\omega}$  and  $di/dt$  provides valuable information on the system: (i) the sign of  $\dot{\omega}$  constrains the spin-orbit angle  $\theta$  (see eq. [7]); (ii) the ratio of  $\dot{\omega}$  and  $di/dt$  yields a relation between  $\theta$  and  $\Phi$ ; (iii) the angle  $\theta_{sn}$  is a function of  $\theta$ ,  $\Phi$ , and  $i$ . Knowing  $i$  and by choosing a reasonable range of  $\theta_{sn}$  (e.g., for the PSR J0045–7319 system: since  $v_{rot}$  must be smaller than the breakup limit  $\simeq 512 \text{ km s}^{-1}$ , we have  $|\sin \theta_{sn}| \lesssim 113/512 = 0.22$ ), we obtain another relation between  $\theta$  and  $\Phi$ ; (iv) With the angles determined from (i)–(iii), the observed values of  $\dot{\omega}$  and  $di/dt$  then constrain the stellar structure and rotation rate of the companion. In addition, long-term timing observations will measure various angles in addition to  $\dot{\omega}$  and  $di/dt$ , yielding additional constraints on the system parameters (see discussion following eq. [9]).

Other effects may prove important for these systems, including the apsidal motion resulting from static tide and general relativity. The dynamical tide (§4) may induce measurable changes in  $P_{orb}$  and  $e$ . However, a detailed theoretical treatment of this effect is complicated by the rapid rotation of the companion star.

The information obtained from the systems can have important implications for the evolution of neutron star binaries. For example, if mass transfer in the presupernova binary forces  $\mathbf{S}$  to be parallel to  $\mathbf{L}$  (a very likely scenario), then a nonzero spin-orbit angle in the pulsar/main-sequence star system implies that the supernova gave the neutron star a kick velocity out of the original orbital plane. From the values of  $\theta$  and  $e$  of the current system (assuming that circularization and spin-orbit alignment are not efficient in the current system), one may actually constrain the kick velocity. Cordes & Wasserman (1984) discussed how such kicks might misalign the neutron star spin from the orbital angular momentum in PSR 1913+16, giving rise to measurable geodetic precession.

### 5.2. X-Ray Binaries

Insight into orbital plane precession might prove important for accreting X-ray pulsars as well. Apsidal motion has been searched for in eccentric accreting systems. In particular, the  $2\sigma$  upper limit on the apsidal motion in the eccentric 8.9 day binary Vela X-1 (which contains a supergiant) is  $\dot{\omega} = 1.6 \text{ yr}^{-1}$  (Deeter et al. 1987). Tamura et al. (1992) claimed a detection of apsidal motion in the eccentric Be system 4U 0115+63 at the level  $\dot{\omega} = 0.030 \pm 0.016 \text{ yr}^{-1}$ . More recent observations of this source with the BATSE instrument (Cominsky, Roberts, & Finger 1994) contradict the claim of Tamura et al. (1992), finding no evidence for apsidal motion. However, these measurements could be biased by the fact that  $a_x \sin i$  was assumed constant.

The less accurate arrival times make the search for orbital plane precession in the accreting X-ray pulsars more difficult than for radio pulsars. However, the orbital parameters are sufficiently accurate that one can search for orbital precession through temporarily separated measurements of  $a_x \sin i$ , the projected size of the orbit for the X-ray pulsar. The system 4U 0115+63, which orbits a Be-type star with  $P_{orb} = 24$  days and has  $e = 0.34$ , may experience  $\Delta i \simeq 6 \times 10^{-3}$  rad over a 17 yr baseline (from eq. [8] assuming a  $10 M_{\odot}$  main-sequence star with radius  $R = 6 R_{\odot}$ ,  $k = 0.01$  and rotating slowly enough,  $\hat{\Omega}_s \simeq 0.05$ , or accidentally having  $\sin^2 \theta$  close to  $\frac{2}{3}$  so as not to violate the upper limit on  $\dot{\omega}$  from Cominsky et al. 1994). This is a factor of 6 larger than the fractional error on  $a_x \sin i$  measured by Rappaport et al. (1978) and may well allow for a very sensitive measurement of the rotation of the Be star in this system.

We thank Roger Blandford and Sterl Phinney for helpful discussion. This work has been supported in part by NASA grants NAGW-2394 to Caltech and NAG5-2819 to the University of California, Berkeley. L. B. was supported as a Compton Fellow at Caltech through NASA grant NAG5-2666 during part of this work. V. M. K. thanks Dave Van Buren for useful discussions, is supported by a Hubble Fellowship through grant number HF-1061.01-94A from the Space Telescope Science Institute, which is operated by the Association of Universities for Research in Astronomy, Inc., under NASA contract NAS5-26555, and carried out research at the Jet Propulsion Laboratory, California Institute of Technology.

### REFERENCES

- Barker, B. M., & O'Connell, R. F. 1975, *ApJ*, 199, L25  
 Bell, J. F., Bessell, M. S., Stappers, B. W., Bailes, M., & Kaspi, V. 1995, *ApJ*, 447, L117  
 Claret, A., & Gimenez, A. 1992, *A&AS*, 96, 255  
 ———. 1993, *A&A*, 277, 487  
 Cominsky, L., Roberts, M., & Finger, M. H. 1994, in *The Second Compton Symposium*, ed. C. E. Fichtel, N. Gehrels, & J. P. Norris (New York: AIP), 294  
 Cordes, J. M., & Wasserman, I. 1984, *ApJ*, 279, 798  
 Cowling, T. G. 1938, *MNRAS*, 98, 734  
 Deeter, J. E., Boynton, P. E., Lamb, F. K., & Zylstra, G. 1987, *ApJ*, 314, 634  
 Goldstein, H. 1980, *Classical Mechanics* (2d ed.; New York: Addison-Wesley)  
 Jaschek, C., & Jaschek, M. 1987, *The Classification of Stars* (New York: Cambridge Univ. Press)  
 Johnston, S., et al. 1992, *ApJ*, 387, L37  
 ———. 1994, *MNRAS*, 268, 430  
 Kaspi, V. M., Johnston, S., Bell, J. F., Manchester, R. N., Bailes, M., Bessell, M., Lyne, A. G., & D'Amico, N. 1994, *ApJ*, 423, L43  
 Kaspi, V. M., Manchester, R. N., Bailes, M., & Bell, J. F. 1995a, in *IAU Symp. 165, Compact Stars in Binaries*, ed. J. van Paradijs, E. P. J. van den Heuvel, & E. Kuulkers (Dordrecht: Kluwer), in press  
 Kaspi, V. M., et al. 1995b, in preparation  
 Kochanek, C. S. 1993, *ApJ*, 406, 638  
 Kopal, Z. 1978, *Dynamics of Close Binary Systems* (Dordrecht: Reidel)  
 Kumar, P., Ao, C. O., & Quataert, E. J. 1995, *ApJ*, 449, 294  
 Landau, L. D., & Lifshitz, E. M. 1962, *Classical Theory of Fields* (Oxford: Pergamon)  
 Lee, H. M., & Ostriker, J. P. 1986, *ApJ*, 310, 176  
 Manchester, R. N., Johnston, S., Lyne, A. G., D'Amico, N., Bailes, M., & Nicastro, L. 1995, *ApJ*, 445, L137  
 Papaloizou, J. C. B., & Pringle, J. E. 1982, *MNRAS*, 200, 49  
 Press, W. H., & Teukolsky, S. A. 1977, *ApJ*, 213, 183  
 Rappaport, S., Clark, G. W., Cominsky, L., Joss, P. C., & Li, F. 1978, *ApJ*, 224, L1  
 Schwarzschild, M. 1958, *Structure and Evolution of the Stars* (Princeton: Princeton Univ. Press)  
 Smarr, L. L., & Blandford, R. D. 1976, *ApJ*, 207, 574  
 Tamura, K., Tsunemi, H., Kitamoto, S., Hayashida, K., & Nagase, F. 1992, *ApJ*, 389, 676  
 Taylor, J. H., & Weisberg, J. M. 1989, *ApJ*, 345, 434  
 Unno, W., Osaki, Y., Ando, H., & Shibahashi, H. 1979, *Nonradial Oscillations of Stars* (Tokyo: Univ. Tokyo Press)  
 Zahn, J.-P. 1977, *A&A*, 57, 383  
 ———. 1984, in *Observational Tests of the Stellar Evolution Theory*, ed. A. Maeder & A. Renzini (Dordrecht: Reidel), 379